Journal of Cellular Biochemistry 96:79–88 (2005)

A Global but Stable Change in HeLa Cell Morphology Induces Reorganization of DNA Structural Loop Domains Within the Cell Nucleus

Isy Martínez-Ramos,[1] Apolinar Maya-Mendoza,[1] Patricio Gariglio,[2] and Armando Aranda-Anzaldo[1]*

[1]Laboratorio de Biología Molecular, Facultad de Medicina, Universidad Autónoma del Estado de México, Apartado Postal 428, C.P. 50000, Toluca, Edo. Méx., México
[2]Departamento de Genética y Biología Molecular, CINVESTAV-IPN, Apartado Postal 14-470, C.P. 07000 D.F., México

Abstract DNA of higher eukaryotes is organized in supercoiled loops anchored to a nuclear matrix (NM). The DNA loops are attached to the NM by means of non-coding sequences known as matrix attachment regions (MARs). Attachments to the NM can be subdivided in transient and permanent, the second type is considered to represent the attachments that subdivide the genome into structural domains. As yet very little is known about the factors involved in modulating the MAR–NM interactions. It has been suggested that the cell is a vector field in which the linked cytoskeleton-nucleoskeleton may act as transducers of mechanical information. We have induced a stable change in the typical morphology of cultured HeLa cells, by chronic exposure of the cells to the polar compound dimethylsulfoxide (DMSO). Using a PCR-based method for mapping the position of any DNA sequence relative to the NM, we have monitored the position relative to the NM of sequences corresponding to four independent genetic loci located in separate chromosomes representing different territories within the cell nucleus. Here, we show that stable modification of the NM morphology correlates with the redefinition of DNA loop structural domains as evidenced by the shift of position relative to the NM of the *c-myc* locus and the multigene locus PRM1 → PRM2 → TNP2, suggesting that both cell and nuclear shape may act as cues in the choice of the potential MARs that should be attached to the NM. J. Cell. Biochem. 96: 79–88, 2005.

Key words: DNA replication; DNA topology; nuclear matrix; PRM1 → PRM2 → TNP2 locus; tensegrity

DNA of higher eukaryotes is organized in supercoiled loops anchored to a nuclear substructure commonly known as the nuclear matrix (NM) [Cook et al., 1976; Roti-Roti et al., 1993]. The topological relationship between gene sequences located in the DNA loops and the NM appears to be very important for appropriate nuclear physiology [Jackson and Cook, 1995; Stein et al., 1995]. Indeed, correct repair of DNA damage must include recovery of both the double helix integrity and the complex, third-dimensional DNA topology, otherwise the cell will not survive [Aranda-Anzaldo and Dent, 1997; Aranda-Anzaldo et al., 1999]. The DNA loops are attached to the NM by means of non-coding sequences known as matrix attachment regions (MARs) [Razin, 2001]. So far there is no specific consensus sequence defining a priori a MAR [Boulikas, 1995; Razin, 1997; Singh et al., 1997]. However, those MARs involved in loop attachment to the NM constitute a subset known as LARs [Razin, 2001]. Attachments to the NM can be subdivided in transient, non-high-salt resistant, and permanent, resistant to high-salt extraction [Razin et al., 1995; Razin,

Grant sponsor: CONACYT, México (to A.A.-A.); Grant numbers: 25416-N, 33539-N.

Apolinar Maya-Mendoza's present address is Faculty of Life Sciences, University of Manchester, PO Box 88, Manchester M60 1QD, UK.

*Correspondence to: Armando Aranda-Anzaldo, MD, PhD, Laboratorio de Biología Molecular, Facultad de Medicina, UAEMéx., Apartado Postal 428, C.P. 50000, Toluca, Edo. Méx., México. E-mail: aaa@uaemex.mx

Received 9 November 2004; Accepted 20 December 2004

DOI 10.1002/jcb.20428

1997; Maya-Mendoza and Aranda-Anzaldo, 2003]. The first type has been associated with the transcriptional regulation of genes while the second type is considered to represent the attachments that subdivide the genome into structural domains [Razin, 1997, 2001; Maya-Mendoza et al., 2003]. Moreover, there is evidence that when multiple copies of a specific MAR are present these are used in a selective and discriminatory manner indicating adaptability of the MAR sequence to serve as anchor only when needed. This suggests that a regulatory system exists within the cell to manage how MAR sequences are used [Heng et al., 2004]. It has been suggested that dynamic selectivity in the use of MARs as DNA anchors would modulate both the DNA loop length and the stability of the topological interactions between DNA and the nuclear substructure during development and cell differentiation [Berezney, 1979; Aranda-Anzaldo, 1989].

As yet very little is known about the factors involved in selecting, establishing, and modulating the MAR/LAR–NM interactions. However, it has been suggested that the cell is a vector field in which the linked cytoskeleton–nucleoskeleton may act as coordinated transducers of mechanical information [Aranda-Anzaldo, 1989] and currently the concept of cell tensegrity incorporates the previous suggestion [Pienta and Coffey, 1991] for which there is already important experimental evidence [Maniotis et al., 1997]. Some models predict that permanent changes in cell shape must lead to modified mechanical interactions within the cell and this would lead to structural changes within the cell nucleus resulting in redefinition of DNA loop domains [Aranda-Anzaldo, 1989]. In order to test this hypothesis, we have induced a radical but stable change in the typical morphology of cultured HeLa cells, by chronic exposure of the cells to the polar compound dimethylsulfoxide (DMSO) that is known to induce significant changes in the cell differentiation state in many cell types [Sato et al., 1971; Tanaka et al., 1975; Viza et al., 1991, 1992]. Thus, using a PCR-based method for mapping the position of any DNA sequence relative to the NM [Maya-Mendoza and Aranda-Anzaldo, 2003; Maya-Mendoza et al., 2004], we have monitored the position relative to the NM of sequences corresponding to four independent genetic loci located in separate chromosomes and as such, representing different territories within the cell nucleus [Cremer and Cremer, 2001]. Here, we show that stable modification of the NM morphology correlates with the redefinition of DNA loop structural domains as evidenced by the shift of position relative to the NM of two loci: the *c-myc* locus and the multigene locus PRM1 → PRM2 → TNP2. Indeed, a sequence internal to this 40 kb locus, located in the spacer between the *PRM1* and *PRM2* genes (very close to the *PRM2* gene 5′ end), shifts from a distal to a very proximal relative position to the NM. Moreover, such a positional change is consequence of establishing new high-salt resistant interactions between the locus and the NM, suggesting that both cell and nuclear shape may act as cues in the choice of the potential MAR/LARs that should be attached to the NM.

MATERIALS AND METHODS

Cells

HeLa cells (from ATTC, Manassas, VA) were grown in DMEM medium plus 5% fetal calf serum, penicillin 40 U/ml, streptomycin sulfate 50 μg/ml and incubated at 37°C in 5% CO_2.

DMSO Treatment

HeLa cells were resuspended in fresh DMEM medium plus fetal calf serum and antibiotics supplemented with 0.5% DMSO (methyl sulfoxide HPLC grade, Sigma-Aldrich, St. Louis, MO). The cells were grown in petri dishes for 72 h until the culture reached confluence. Cells were harvested and resuspended in fresh medium supplemented with 1% DMSO and grown for 72 h. Then harvested and resupended in fresh medium with 2% DMSO and grown for 72 h. Cell viability was assessed by Trypan blue exclusion and only cells from cultures showing more than 70% viability were harvested and seeded in new petri dishes with medium supplemented with 2% DMSO. The gradual morphological change of the cells was monitored under the microscope. After 6 weeks of culture in 2% DMSO basically 100% of cells showed a stable change to an elongated, fibroblast-like morphology.

Preparation of Nucleoids

The DNA loops plus the NM constitute a "nucleoid," a very large nucleoprotein aggregate. In all cases we used confluent cultures as the source of cells for preparing nucleoids.

Nucleoids were prepared as previously described [Maya-Mendoza and Aranda-Anzaldo, 2003]. Briefly: both control and DMSO-treated cells are detached from the culture dish in the same gentle way by 5 min incubation in prewarmed PBS-A containing 0.2 g/L of EDTA without proteolytic enzymes and using very mild scrapping with a rubber policeman. Harvested and washed cells are suspended in ice-cold phosphate buffered saline without Ca^{2+} and Mg^{2+} (PBS-A). Aliquots of 50 μl containing between $2-5 \times 10^5$ cells are gently mixed with 150 μl of a lysis solution containing: 2.6M NaCl; 1.3 mM EDTA; 2.6 mM Tris; 0.6% Triton X-100, pH 8.0. After 20 min at 4°C, the mixture is overlaid on sucrose "step" gradients that contain: 0.2 ml of 30% sucrose under 0.6 ml 15% sucrose. Both sucrose layers contain 2.0M NaCl; 1.0 mM EDTA; 10 mM Tris, pH 8.0. The gradients are spun at 4°C in a microfuge for 4 min at 10,000 rpm (9,000*g*). The nucleoids form a white aggregate that usually sediments to the interface between the two layers of sucrose. These nucleoids are carefully recovered in a volume ranging from 200 to 300 μl, using a 1 ml micropipette. The recovered nucleoid suspension is washed in 14 ml of PBS-A at 4°C for 4 min at 3,000 rpm (1,500*g*). After this centrifugation step the nucleoids form a rather cloudy and fluid pellet at the bottom of the tube. The full cloud of nucleoids is recovered in a volume ranging from 200 to 300 μl (the typical nucleoid concentration is 2.5×10^5 in 200 μl).

DNase I Digestion of Nucleoid Samples

Stocks of DNase I (deoxyribonucleate 5′-oligonucleotidohydrolase) from Sigma-Aldrich, were prepared by dilution in 0.3M NaCl plus glycerol (50:50 vol/vol). Typical stocks contained 460 U kunitz/200 μl. DNase I digestion buffer contains 10 mM $MgCl_2$, 0.1 mM dithiothreitol, 50 mM TRIS at pH 7.2. The washed nucleoids are pooled for setting up the DNase I digestion curves (1.5×10^6 in roughly 1.2 ml of PBS-A), and mixed with DNase I digestion buffer (usually 5 ml of digestion buffer for each 1.2 ml of nucleoid suspension). DNase I digestions (0.5 U/ml) are carried out at 37°C. Each digestion time-point aliquot contains 2.5×10^5 nucleoids. The stop buffer contains 0.2M EDTA and 10 mM TRIS at pH 7.5. DNase I digestion reactions are stopped by adding enough stop buffer so as to achieve an EDTA concentration of 30 mM.

Electroelution of Nuclease-Digested Nucleoids

In order to remove DNA fragments non-specifically bound to the NM, all non-radioactive samples of partially nuclease-digested nucleoids were resuspended in 0.3 ml of TBE 0.5× and loaded in a dialysis bag (membrane Spectra/Por 7 MWCO 50,000, diameter 7.5 mm, 0.45 ml/cm, from Spectrum Laboratories, Inc., Los Angeles, CA). The dialysis bag was immersed in a horizontal electrophoresis chamber containing 50 ml of 0.5× Tris-Borate-EDTA (TBE) buffer pH 8. The bag was fixed perpendicular to the axis of the electric current flow. The sample was electroeluted at 100 V for 2 h (the running buffer was changed after the first hour so as to avoid overheating). The material within the bag was recovered and centrifuged 10 min at 10,000 rpm (9,000g) at 4°C. The pellet was further washed twice in double-deionized water (dd-H_2O) at a ratio of 1:10 vol/vol (9,000g for 10 min at 4°C). The pellet was resuspended in 100 μl of dd-H_2O to be used as template for PCR.

Estimation of NM-Bound DNA

HeLa cells either control or DMSO-treated were grown for 48 h in medium supplemented with ^{3}H-thymidine (^{3}H-Tdr) at 0.02 μCi/ml. The ^{3}H-labeled cells were harvested, washed and used for preparing nucleoids that were subjected to digestion with DNase I. Triplicate aliquots were collected at the specified digestion times, they were not electroeluted but washed as previously described for removing any DNA fragments non-specifically bound to the NM [Maya-Mendoza and Aranda-Anzaldo, 2003], treated with 5% ice-cold TCA and then filtered and washed with ethanol and distilled water. The filters were counted for radioactivity in a toluene-based scintillant.

PCR Amplification

Standard PCR was carried out using Taq polymerase (GIBCO-BRL, Life Technologies, Paisley, UK) and NM-bound DNA (nucleoids) as template for amplification of predetermined sequences, in an Applied Biosystems GeneAmp PCR System 2400 thermocycler. For initial standardization the PCR was maintained within the linear range of amplification. PCR products were visualized in agarose gels stained with ethidium bromide (0.5 μg/ml), recorded and analyzed using a Eastman Kodak 1D Image Analysis Software 3.5 (Rochester, NY). The

identity of all the amplified sequences was confirmed by restriction analysis with the appropriate restriction enzymes.

Genomic Primers

β-*actin* (universal actin, accession number M10277). 5′-AACACCCCAGCCATGTACG (S); 5′-ATGTCACGCACGATTTCCC (A). Location: exon 4. Amplicon size: 253 bp. Chromosome location: 7pter-q22. Human β-*globin* (accession number M24868). 5′-GAAGAGCCAAGGACAGGTAC (S); 5′-CAACTTCATCCACGTTCACC (A). Location: spacer δ-β and part of first β-*globin* exon. Amplicon size: 270 bp. Chromosome location: 11p15.5. Human *c-myc* gene (accession number J00120). 5′-TTCTACTGCGACGACGAGGAG (S); 5′-AGGGTAGGGGAAGACCACCGA (A). Location: exon 2. Amplicon size: 528 bp. Chromosome location: 8q24. Marker PRM2 (Human locus PRM1 → PRM2 → TNP2, accession number U15422). 5′-AGGGGTAGAGGCTGCTATGAT (S). 5′-CAGCAGCAAACAGTTCCCTAATAG (A). Location: spacer between *PRM1* and *PRM2* genes, nucleotides 19209–19388. Amplicon size: 180 bp. Chromosome location: 16p13.13.

Amplification Programs

All pairs of primers used at 25 pmol. For β-*actin* and β-*globin*: initial denaturation step at 94°C for 5 min, denaturation step 94°C for 45 s, annealing at 56°C for 30 s, and extension at 72°C for 1 min for 35 cycles, with a final extension at 72°C for 10 min. For *c-myc*: initial denaturation step at 94°C for 5 min, denaturation step 94°C for 30 s, annealing at 65°C for 1 min, and extension at 72°C for 1 min for 35 cycles, with a final extension at 72°C for 10 min. For PRM2 marker: initial denaturation step at 94°C for 5 min, denaturation step 94°C for 1 min, annealing at 55°C for 2 min, and extension at 72°C for 2 min for 40 cycles, with a final extension at 72°C for 10 min.

RESULTS

HeLa cells were progressively exposed to increasing concentrations of DMSO in the culture medium from 0.5% to 2% (see "Materials and Methods"). The cells showed a gradual change in morphology going from the typical rhomboid–tetrahedral shape (Fig. 1A) to an elongated, fibroblast-like morphology (Fig. 1B) that became quite stable after 6 weeks of growth in 2% DMSO. The change in morphology was accompanied by significant changes in cell behavior in culture, since the typical HeLa cells grow rather fast, pile up, and detach rather easily from the culture dish, showing no contact inhibition of cell growth. On the other hand, the fibroblast-like HeLa cells grow quite slowly, attach tightly to the culture dish, do not pile up and clearly show contact inhibition of growth. These cellular features, rather common in transformed cells chronically exposed to DMSO, have been interpreted as evidence for "normalization" of the differentiation state of the transformed cells [Sato et al., 1971; Tanaka et al., 1975; Viza et al., 1991, 1992]. Yet, the dramatic

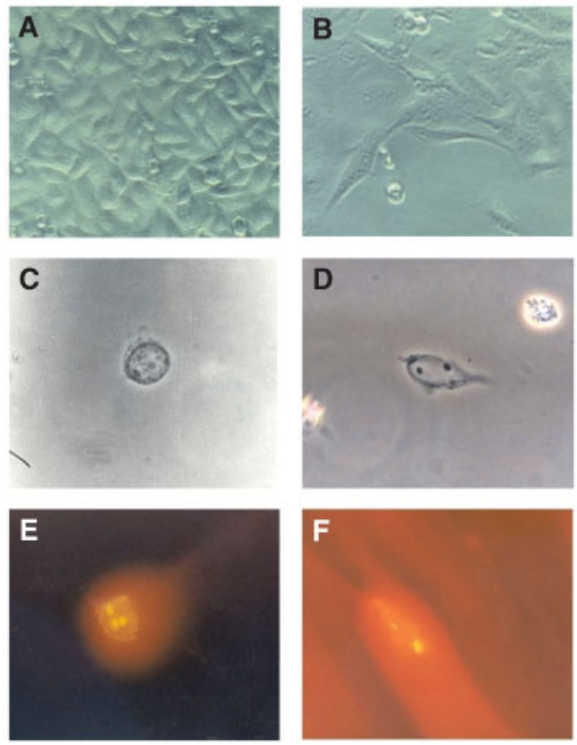

Fig. 1. Morphology of control and dimethylsulfoxide (DMSO)-treated HeLa cells. **A**: Typical morphology of control HeLa cells. **B**: Morphology of HeLa cells after 6 weeks of chronic treatment with 2% DMSO. **C**: Phase contrast micrograph showing the typical round morphology of the nuclear matrix (NM) from a control HeLa cell. **D**: Phase contrast micrograph showing the typical elongated morphology of the NM from a DMSO-treated HeLa cell. **E**: Fluorescence micrograph of a control HeLa nucleoid treated with 40 μg/ml of ethidium bromide. Note the homogeneous halo formed by the relaxed DNA loops around the NM contour. **F**: Fluorescence micrograph of a nucleoid from a DMSO-treated HeLa cell exposed to 40 μg/ml of ethidium bromide. Note the comet tail-like loop DNA halo projecting from the elongated NM and the significant presence of free DNA released from the NM by the ethidium bromide (magnification 200× A and B; 400× C, D, E, F).

morphological change observed in HeLa cells after chronic DMSO treatment in no way corresponds to the typical morphology of non-transformed, epithelial cells from the uterine cervix that are the precursors from which the HeLa tumor cells arose. Thus, we cannot affirm that a true normalization in the cell differentiation state is taking place. Nevertheless, the DMSO-induced change in cell shape becomes non-dependent on DMSO itself, since HeLa cells previously grown for 7 weeks in 2% DMSO preserved their fibroblast-like shape and modified culture behavior at least for up to 21 days of further growth in DMSO-free medium. Moreover, fibroblast-like HeLa cells were frozen, stored, and then thawed and re-grown in DMSO-free medium, but they kept the fibroblast-like shape and normalized culture behavior at least for 2 weeks of further culture.

The change in overall cell shape is also observed at the level of the NM, since the typical HeLa cell NM is rather round or circle-like (Fig. 1C) while in Hela cells chronically exposed to 2% DMSO the NM has a rather elongated shape (Fig. 1D). This change in NM shape correlates with the properties of the corresponding nucleoids resulting from the high-salt extraction of the cells and which consist of the NM plus the naked DNA loops anchored to it. This fact confirms that the significant morphological change of the NM has occurred in cell culture and is not the consequence of detachment of the cells from the culture dish. Moreover, if there is a transient change in cell morphology due to detachment from the culture dish such a change leaves no permanent evidence as shown by the stable elongated morphology of the NM from DMSO-treated cells which is actually isolated in suspension. In typical HeLa cell nucleoids exposure to a DNA-intercalating agent such as ethidium bromide (EtBr) leads to unwinding of the DNA loops that form a well-defined halo around the NM perimeter (Fig. 1E). However, the DMSO-modified HeLa nucleoids become quite sensitive to the action of EtBr, since a similar concentration of the intercalating agent induces not only the unwinding but also the actual release of DNA from the NM. Thus, the DMSO-modified nucleoids show comet-like tails of DNA projecting from the NM contour, and the field under the microscope becomes quickly saturated with free DNA stained with EtBr, indicating that the interactions between DNA and the NM are on the whole more labile in the DMSO-treated nucleoids (Fig. 1F).

The high sensitivity of the DNA to EtBr in DMSO-treated nucleoids is mirrored by its sensitivity to digestion by DNase I. Control HeLa nucleoids incubated with a finely adjusted concentration of DNase I [Maya-Mendoza and Aranda-Anzaldo, 2003], show a smooth and reasonably slow kinetics of DNA digestion in time, that leaves after 30 min of digestion some 17% of the total DNA unscathed and attached to the NM (Fig. 2). However, the DNA from DMSO-treated nucleoids shows a much faster kinetics of DNA digestion with DNase I, even though the amount of NM-bound DNA remaining after 30 min of digestion is about the same (14%) as in the control (Fig. 2). In high-salt extracted nucleoid preparations, the DNA is practically devoid of histones and other chromatin proteins, under such condition the naked loop DNA shows a sensitivity to non-specific nucleases that is inversely proportional to its location relative to the NM, the DNA closest to the NM being more resistant to endonuclease digestion [Razin et al., 1995; Maya-Mendoza and Aranda-Anzaldo, 2003; Maya-Mendoza et al., 2004].

We chose four different sequences corresponding to four separate loci located in different chromosomes, for mapping their position relative to the NM. All sequences were within the 180–528 bp range, therefore shorter than the average size of the DNA fragments liberated from the nucleoids by non-specific nucleases, estimated at 0.8 kb [Berezney and Buchholtz, 1981; our own unpublished results]. The chosen sequences are located either within the actual gene (β-*actin*, β-*globin*, *c-myc*) or in the spacer DNA very close to the 5′ promoter (PRM2) (see "Materials and Methods"). We chose such sequences because they belong to constitutive (β-*actin*), disregulated (*c-myc*), and non-expressed genes (β-*globin*, *PRM2*) in HeLa cells, besides being located in separate chromosomes representing different territories within the cell nucleus [Cremer and Cremer, 2001]. The mapping protocol has been thoroughly described [Maya-Mendoza and Aranda-Anzaldo, 2003; Maya-Mendoza et al., 2003, 2004; Iarovaia et al., 2004] and it involves the progressive detachment of DNA from the nuclear substructure by digestion with a carefully adjusted concentration of DNase I followed by specific procedures to remove any DNA fragment

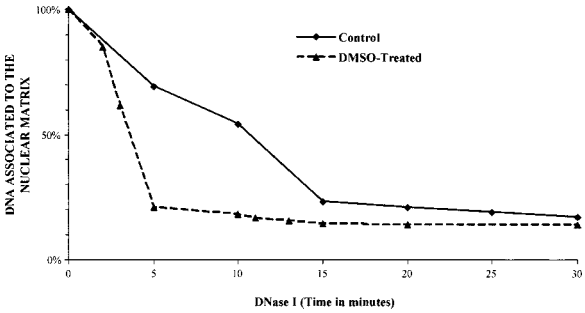

Fig. 2. Kinetics of digestion with DNase I (0.5 U/ml) of total DNA from nucleoids from control or DMSO-treated HeLa cells. Each point is the average of triplicates (SD $\leq$ 3%).

detached from the NM and then carrying direct PCR-amplification of the specific target sequences on NM-bound templates. In our mapping protocol the actual intensity of the amplicon signal at each particular DNase I digestion time is non-relevant because the PCR is not quantitative. The amplicon signals are scored either as positive or negative, based on whether they are detected or not by a digital image analysis system, since we are monitoring the average DNA loop arrangement in a large number of nucleoids and so the observed degree of resistance to digestion of a given DNA sequence corresponds to its average across the large nucleoid population analyzed. Thus, the critical parameter evaluated is whether a particular DNA sequence can be amplified or not after a given time of nucleoid-DNA digestion with DNase I.

The PCR amplification results are calibrated using as a gauge the percentage of total DNA remaining associated with the NM at each digestion time and according to the specific kinetics for nucleoid-DNA digestion (Fig. 2). The Tables I and II show the mapping results that were exactly the same in at least three separate experiments. With such results we can define positional windows relative to the NM for the sequences studied. The upper value on each window corresponds to the percentage of total DNA associated with the NM at which each specific amplicon was last detected. The lower value corresponds to the percentage of total DNA associated with the NM at which each specific amplicon was not detected anymore. Hence, the specific DNA sequence corresponding to each amplicon is expected to be located, on average, within the interval defined by such values (Table III). The mapping results clearly show that each sequence has a specific position relative to the NM in control HeLa nucleoids. Moreover, such a control position remains the same for both the β-*actin* and β-*globin* sequences in the DMSO-treated nucleoids. However, both the *c-myc* and PRM2 sequences shift their position relative to the NM in DMSO-treated nucleoids, becoming closer to the NM. Being quite notable the phenomenon in the case of the PRM2 sequence (Table III).

TABLE I. DNase I Digestion Time at Which the Corresponding Amplicon Is Observed (Control HeLa Nucleoids)

Time (min)	β-*Actin*	β-*Globin*	*c-myc*	PRM2
0	+	+	+	+
5	+	+	+	+
10	+	+	+	+
11	n.d.	n.d.	+	+
13	n.d.	n.d.	+	−
15	+	+	−	−
20	+	+	−	−
25	n.d.	−	n.d.	n.d.
30	+	−	−	−

Nucleoids were digested with DNase I (0.5 U/ml) for the specified times. Remaining NM-bound DNA was directly used as template for amplification with the appropriate primers. PCR products were visualized in agarose gels stained with ethidium bromide (0.5 μg/ml), recorded and analyzed using a Kodak 1D Image Analysis Software 3.5; (+) indicates that the amplicon was detected by the image analysis software; (−) indicates that the amplicon was not detected by the image analysis software. Amplification results were exactly the same in at least three separate experiments, n.d., not done.

DISCUSSION

Chronic treatment of HeLa cells with DMSO induces a dramatic but stable change in cell

TABLE II. DNase I Digestion Time at Which the Corresponding Amplicon Is Observed (DMSO-Treated HeLa Nucleoids)

Time (min)	β-*Actin*	β-*Globin*	*c-myc*	PRM2
0	+	+	+	+
2	n.d.	n.d.	+	+
3	n.d.	n.d.	+	+
5	+	+	+	+
10	+	−	−	+
15	+	−	−	+
20	+	−	n.d.	+
30	+	−	−	+

Nucleoids were digested with DNase I (0.5 U/ml) for the specified times. Remaining NM-bound DNA was directly used as template for amplification with the appropriate primers. PCR products were visualized in agarose gels stained with ethidium bromide (0.5 μg/ml), recorded and analyzed using a Kodak 1D Image Analysis Software 3.5; (+) indicates that the amplicon was detected by the image analysis software; (−) indicates that the amplicon was not detected by the image analysis software. Amplification results were exactly the same in at least three separate experiments, n.d., not done.

TABLE III. Positional Windows Corresponding to Percentage of NM-Bound DNA Within Which the Specific Amplified Sequences Are Located

	Control HeLa nucleoids	DMSO-treated nucleoids
β-*Actin*	17 > 0	14 > 0
β-*Globin*	21–19	21–17
c-myc	35–23	21–17
PRM2	47–35	14 > 0

Positional windows were established by correlating the data in Tables I and II with the specific DNase I digestion kinetics (Fig. 2). The upper value on each window corresponds to the percentage of total DNA associated with the NM at which each specific amplicon was last detected. The lower value corresponds to the percentage of total DNA associated with the NM at which each specific amplicon was not detected anymore. The specific DNA sequence corresponding to each amplicon is expected to be located, on average, within the interval defined by such values. Because nucleoid DNA digestions were carried out up to 30 min a significant percentage of DNA remained bound to the NM after that time (≥14%), thus in some cases the specific amplicon signal was never extinguished and so (>) indicates that the specific sequence is likely to be located between the upper boundary value and a lower boundary greater than zero.

shape that also is accompanied by a stable morphological change of the NM. The exact mechanism by which DMSO induces such changes also previously observed in different cell types, is not known. Indeed, DMSO acts pleiotropically on cells being able to affect organelle biogenesis [Sato et al., 1971], DNA transition temperature [Terada et al., 1978], cytoskeleton and nucleoskeleton assembly [Fukui and Katsumaru, 1979; Osborn and Weber, 1980], cell transcription and/or translation and as such endogenous virus assembly [Viza et al., 1989, 1992]. Nevertheless, the observed shift from a rhomboidal to an elongated, fibroblast-like shape in HeLa cells necessarily implies a radical adjustment in the mechanical interactions between the cytoskeleton and the nucleoskeleton. Moreover, the interactions between DNA and the NM are clearly modified in the DMSO-treated cells, since the loop DNA becomes more fragile and is easily released from the NM by EtBr (Fig. 1F). This correlates with the fact that the largest part of the naked nuclear DNA becomes more sensitive to DNase I, though the relative proportion of DNA closely attached or protected by its proximity to the NM remains about the same in both control and DMSO-treated nucleoids (Fig. 2). The faster kinetics of DNase I digestion observed in DMSO-treated nucleoids is evidence of significant changes in the DNA loop topology. Indeed, in high-salt extracted nucleoid preparations the two parameters that hinder DNase I action are steric hindrance due to proximity to the NM that acts as a barrier protecting naked DNA from the endonuclease, and supercoiling that is a structural barrier against the action of enzymes that hydrolyze the DNA backbone by a single-strand cleavage mechanism, such as DNase I [Lewin, 1980; Razin et al., 1995]. Both factors only confer relative but not absolute endonuclease-resistance to DNA and so the stochastic action of the non-specific endonuclease implies that all sequences might be targeted to some extent at all levels of total nucleoid-DNA digestion. However, factors that result in loss of DNA supercoiling and/or excess of nicked single-stranded DNA, such as intense DNA replication or virus-induced DNA breaks followed by DNA loop unwinding, lead to a fast kinetics of DNase I digestion even though there is always a significant percentage of DNA close to the NM that is highly resistant to the endonuclease [Aranda-Anzaldo and Dent, 1997; Aranda-Anzaldo, 1998].

Among the four loci mapped, two of them, non-related and located in different chromosome territories (*c-myc* and PRM2) show a significant shift towards a position closer to the NM in DMSO-treated nucleoids. This is observed in stable, non-synchronized, contact inhibited cell cultures. In contrast, a larger set of genes analyzed in synchronized replicating cells in vivo shows that with no exception the genes become proximal to the NM during the S phase. But such positional shifts towards the NM shown by most genes are transient and the genes regain their original position when the cells return to G_0 [Maya-Mendoza et al., 2003, 2004]. Such transient gene positional shifts support the notion that DNA replication in vivo occurs at fixed sites located upon the NM, through which the DNA reels in instead of being copied by long-distance tracking polymerases [Cook, 1999]. Therefore, the fact that in DMSO-treated confluent cells some genes become proximal to the NM while others remain in their original position corresponding to that observed in confluent control cells, indicates that we are observing a phenomenon that is not related to the replicating status of the cells. However, the changes of position observed in the *c-myc* and PRM2 loci seem to imply that potential MARs become actually bound to the

NM and in a high-salt resistant fashion, meaning the establishment of new structural DNA attachments to the NM that were not present in the control HeLa cells.

It is particularly noticeable the shift in position shown by the PRM2 sequence. Indeed, the *PRM2* gene is part of the PRM1 → PRM2 → TNP2 multigene locus that is specifically haploid-expressed in human sperm cells, during spermiogenesis [Wykes et al., 1995; Steger et al., 2000]. The locus nucleotide sequence and chromatin structure has been fully characterized [Choudhary et al., 1995; Kramer and Krawetz, 1996; Wykes and Krawetz, 2003] and it is particularly interesting that three different MARs have been identified within the 40 kb region encompassing the locus (Fig. 3A). Two sperm-specific MARs, one towards the 5′ region of the locus and bounded by nucleotide positions 8,818–9,760, some 5,125 bp upstream of the *PRM1* gene 5′ end, and a second towards the 3′ region of the locus and bounded by nucleotides 32,586–33,536, some 4,154 bp downstream of the *TNP2* gene [Kramer and Krawetz, 1996]. The third MAR is functional in somatic cells and is located in the 3′ region of the locus (centered at nucleotide 38,200) some 9.5 kb downstream of the *TNP2* gene and some 2.5 kb upstream of the *SOCS-1* gene that is the next gene downstream of the PRM1 → PRM2 → TNP2 multigene locus [Kramer et al., 1998; Wykes and Krawetz, 2003]. In sperm cells it has been shown that the 5′ attachment of this multigene locus to the NM is mediated by the MAR upstream of the *PRM1* gene, but this MAR is not functional in normal somatic cells [Kramer and Krawetz, 1996].

The average DNA loop size in HeLa cells has been estimated at 86 kb [Jackson et al., 1990], thus the length of the loop from base to tip must be around 43 kb. Our mapping results show that the positional window of the PRM2 sequence shifts from 47% to 35% to 14% or less of residual NM-bound DNA (Table III). The difference from 35% to 14% is 21% and this figure roughly corresponds to 9 kb of loop DNA length. Interestingly, the distance between the 5′ end of the PRM2 mapped sequence (nucleotide 19,209) and the 3′ end of the region where is located the 5′ sperm-specific MAR (nucleotide 9,760) is

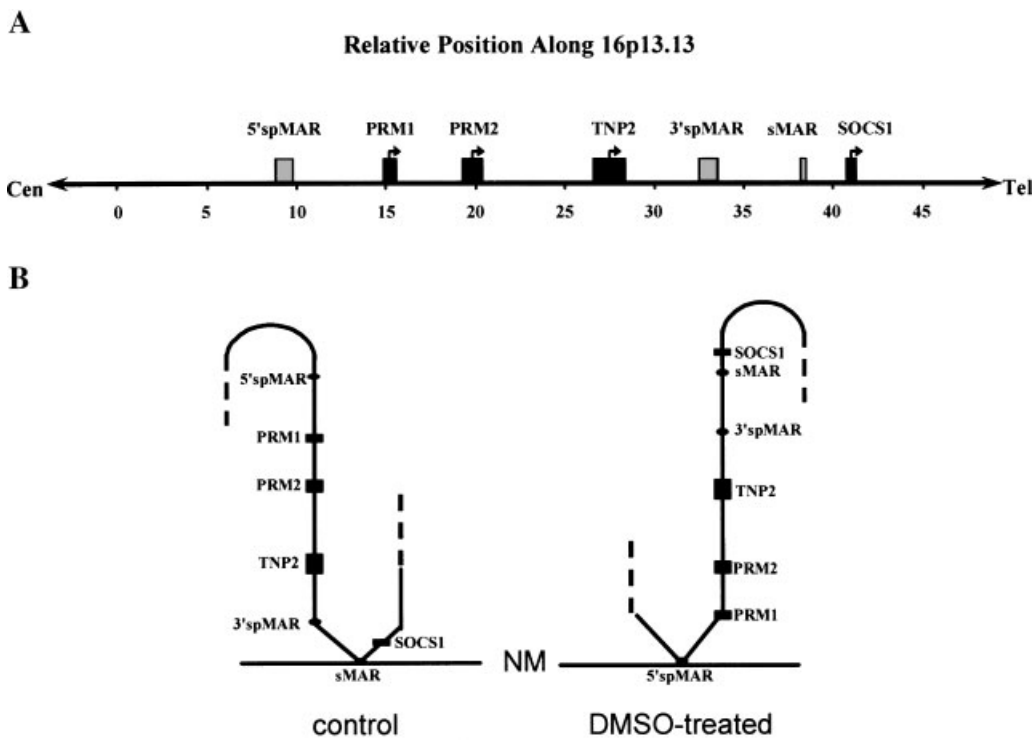

Fig. 3. **A**: Map showing the relative position of the genes (PRM1 → PRM2 → TNP2 and SOCS1) and the mapped sperm-specific (sp) and somatic (s) MARs within a 45 kb region along the human chromosome 16. **B**: Model showing the difference between control and DMSO-treated HeLa cell nucleoids in the relative position to the NM of the elements shown in A.

9,449 bp. Moreover, the somatic MAR located in the 3′ region of the locus is some 19 kb from the 5′ PRM2 sequence that in control HeLa nucleoids maps to 47%–35% of total NM-bound DNA. This positional window is equivalent to a range of 20–15 kb from the attachment to the NM. Thus, our results are consistent with the model depicted in Figure 3B: in control HeLa cells the PRM1 → PRM2 → TNP2 locus is attached to the NM by means of the somatic 3′ MAR that is close to the 5′ end of the *SOCS-1* gene and is high-salt resistant in somatic cells [Kramer et al., 1998]. In that situation the 5′ end of the *PRM2* gene lays some 20–15 kb from the attachment to the NM. In DMSO-treated cells the 5′ sperm-specific MAR attaches in a high-salt resistant fashion to the NM and the somatic 3′ MAR is released. In that situation the 5′ end of the *PRM2* gene shifts to a position closer to the NM, equivalent to some 9–6 kb from the attachment to the NM.

Given the uncertainty about the pleiotropic effects of DMSO upon the HeLa cells, we think that the global change in cell and NM shape induced by DMSO is the simplest explanation for the observed positional changes relative to the NM. Though of course the morphological change may modify the internal cell machinery and some of such modifications might be instrumental in the actual changes in DNA topology within the cell nucleus. Indeed, it is unlikely that cells may stably change their morphology by whichever method without undergoing a correlated change in their physiology. However, from the structural perspective we must take into account that the average DNA loops size shifts from some 60–86 kb in somatic cells [Razin et al., 1995] to some 27 kb in sperm nuclei [Schmid et al., 2001], where the 5′ sperm-specific MAR normally binds to the NM, and this correlates with the significantly reduced size and volume of the sperm nucleus. Moreover, a highly condensed chromatin state is achieved in the sperm nucleus by replacing some 85% of the histones with the smaller and more basic protamines [Schmid et al., 2001]. Our results suggest that the change in cell and NM shape induces that the 5′ sperm-specific MAR firmly binds to the NM in nucleoids from DMSO-treated cells, thus leading to a stable reorganization of the higher-order DNA structure in the region encompassing the PRM1 → PRM2 → TNP2 locus. It is worth mention that the *PRM2* gene remains non-expressed in the HeLa DMSO-treated cells, while the *c-myc* gene is expressed at the same level than in the control HeLa cells (our unpublished results), which was likely to be expected, considering that it has been shown that the positions of genes relative to the NM mediated by high-salt resistant structural attachments are not related to transcription status and so the genes display transcription levels that are independent of their position relative to the NM [Maya-Mendoza et al., 2003, 2004]. Moreover, tissue specific expression of genes such as *PRM2* depends on very specific local chromatin changes mediated by a number of chromatin-modifying and DNA-binding proteins, some that are likely to be available only in the specific differentiated cells where the particular gene expression is needed [Ha et al., 1997; Kramer et al., 1998]. Nevertheless, our results support the hypothesis that mechanical information transduced by cytoskeleton and nucleoskeleton modifies the topological relationships between the chromatin and the nuclear substructure [Aranda-Anzaldo, 1989]. Thus, mechanical effects resulting from the interactions of groups of cells organized as tissues in vivo may act as cues for reorganizing the higher-order DNA structure within the cell nucleus and so guiding the process of cell differentiation.

ACKNOWLEDGMENTS

Isy Martínez-Ramos was a graduate student within the Molecular Biomedicine M.Sc. program at CICATA-IPN, México. We thank Juan Carlos Rivera-Mulia for helping with graphs and figures.

REFERENCES

Aranda-Anzaldo A. 1989. On the role of chromatin higher-order structure and mechanical interactions in the regulation of gene expression. Speculat Sci Technol 12:163–176.

Aranda-Anzaldo A. 1998. The normal association between newly-replicated DNA and the nuclear matrix is abolished in cells infected by herpes simplex virus type 1. Res Virol 149:195–208.

Aranda-Anzaldo A, Dent MAR. 1997. Loss of DNA loop supercoiling and organization in cells infected by herpes simplex virus type 1. Res Virol 148:397–408.

Aranda-Anzaldo A, Orozco-Velasco F, García-Villa E, Gariglio P. 1999. p53 is a rate-limiting factor in the repair of higher-order DNA structure. Biochem Biophys Acta 1446:181–192.

Berezney R. 1979. Dynamic properties of the nuclear matrix. In: Busch H, editor. The cell nucleus. Orlando: Academic Press. pp 413–456.

Berezney R, Buchholtz LA. 1981. Dynamic association of replicating DNA fragments with the nuclear matrix of regenerating liver. Exp Cell Res 132:1–13.

Boulikas T. 1995. Chromatin domains and prediction of MAR sequences. Int Rev Cytol 162A:279–387.

Choudhary SK, Wykes SM, Kramer JA, Mohamed AN, Koppitch F, Nelson JE, Krawetz SA. 1995. A haploid expressed gene cluster exists as a single chromatin domain in human sperm. J Biol Chem 270:8755–8762.

Cook PR. 1999. The organization of replication and transcription. Science 284:1790–1795.

Cook PR, Brazell I, Jost E. 1976. Characterization of nuclear structures containing superhelical DNA. J Cell Sci 22:303–324.

Cremer T, Cremer C. 2001. Chromosome territories, nuclear architecture and gene regulation in mammalian cells. Nat Rev Genet 2:292–300.

Fukui Y, Katsumaru H. 1979. Nuclear actin bundles in Amoeba, Dictyostelium and human HeLa cells induced by dimethylsulfoxide. Exp Cell Res 120:451–455.

Ha H, van Wijnen AJ, Hecht NB. 1997. Tissue-specific protein–DNA interactions of the mouse protamine 2 gene promoter. J Cell Biochem 64:94–105.

Heng HHQ, Goetze S, Ye JC, Liu G, Stevens JB, Bremer SW, Wykes SM, Bode J, Krawetz SA. 2004. Chromatin loops are selectively anchored using scaffold/matrix-attachment regions. J Cell Sci 117:999–1008.

Iarovaia O, Shkumatov P, Razin SV. 2004. Breakpoint cluster regions of the *AML-1* and *ETO* genes contain MAR elements and are preferentially associated with the nuclear matrix in proliferating HEL cells. J Cell Sci 117: 4583–4590.

Jackson DA, Cook PR. 1995. The structural basis of nuclear function. Int Rev Cytol 162A:125–149.

Jackson DA, Dickinson P, Cook PR. 1990. The size of chromatin loops in HeLa cells. EMBO J 9:567–571.

Kramer JA, Krawetz SA. 1996. Nuclear matrix interactions within the sperm genome. J Biol Chem 271:11619–11622.

Kramer JA, Adams MD, Singh GB, Doggett NA, Krawetz SA. 1998. A matrix associated region localizes the human SOCS-1 gene to chromosome 16p13.13. Somat Cell Mol Genet 24:131–133.

Lewin B. 1980. Gene expression 2, 2nd edn. New York: John Wiley and Sons. pp 360–362.

Maniotis A, Chen CS, Ingber D. 1997. Demonstration of mechanical connections between integrins, cytoskeletal filaments and nucleoplasm, that stabilize nuclear structure. Proc Natl Acad Sci USA 94:849–854.

Maya-Mendoza A, Aranda-Anzaldo A. 2003. Positional mapping of specific DNA sequences relative to the nuclear substructure by direct polymerase chain reaction on nuclear matrix-bound templates. Anal Biochem 313: 196–207.

Maya-Mendoza A, Hernández-Muñoz R, Gariglio P, Aranda-Anzaldo A. 2003. Gene positional changes relative to the nuclear substructure correlate with the proliferating status of hepatocytes during liver regeneration. Nucleic Acids Res 31:6168–6179.

Maya-Mendoza A, Hernández-Muñoz R, Gariglio P, Aranda-Anzaldo A. 2004. Gene positional changes relative to the nuclear substructure during carbon tetrachloride-induced hepatic fibrosis in rats. J Cell Biochem 93:1084–1098.

Osborn M, Weber K. 1980. Dimethylsulfoxide and the ionophore A23187 affect the arrangement of actin and induce nuclear actin paracrystals in PtK2 cells. Exp Cell Res 129:103–114.

Pienta KJ, Coffey DS. 1991. Cellular harmonic information transfer through a tissue tensegrity-matrix system. Med Hypoth 38:88–95.

Razin SV. 1997. Nuclear matrix and the spatial organization of chromosomal DNA domains. Austin Texas: RG Landes Co. pp 81–109.

Razin SV. 2001. The nuclear matrix and chromosomal DNA loops: Is there any correlation between partitioning of the genome into loops and functional domains? Cell Mol Biol Lett 6:59–69.

Razin SV, Gromova II, Iarovaia OV. 1995. Specificity and functional significance of DNA interaction with the nuclear matrix: New approaches to clarify the old questions. Int Rev Cytol 162B:405–448.

Roti-Roti JL, Wright WD, Taylor YC. 1993. DNA loop structure and radiation response. Adv Radiat Biol 17: 227–259.

Sato T, Friend Ch, de Harven E. 1971. Ultrastructural changes in Friend erythroleukemia cells treated with dimethyl sulfoxide. Cancer Res 31:1402–1417.

Schmid C, Heng HHQ, Rubin C, Ye CJ, Krawetz SA. 2001. Sperm nuclear matrix associaiton of the PRM1 → PRM2 → TNP2 domain is independent of Alu methylation. Mol Hum Reprod 7:903–911.

Singh GB, Kramer JA, Krawetz SA. 1997. Mathematical model to predict regions of chromatin attachment to the nuclear matrix. Nucleic Acids Res 25:1419–1425.

Steger K, Pauls K, Klonish T, Franke FE, Bergmann M. 2000. Expression of protamine-1 and -2 mRNA during human spermiogenesis. Mol Hum Reprod 6: 219–225.

Stein GS, van Wijnen AJ, Stein J, Lian JB, Montecino M. 1995. Contributions of nuclear architecture to transcriptional control. Int Rev Cytol 162A:251–278.

Tanaka M, Levy J, Tarada M, Breslow R, Rifikind RA, Marks PA. 1975. Induction of erythroid differentiation in murine virus infected erythroleukemia cells by highly polar compounds. Proc Natl Acad Sci USA 72:1003–1006.

Terada M, Nudel U, Fibach E, Rifkind RA, Marks PA. 1978. Changes in DNA associated with induction of erythroid differentiation by DMSO in murine erythroleukemia cells. Cancer Res 38:835–840.

Viza D, Aranda-Anzaldo A, Ablashi D, Zompetti C, Salahuddin SZ, Vich JM. 1989. Chemical inducers of cell differentitation inhibit HIV in vitro. AIDS-Forschung 7:349–352.

Viza D, Aranda-Anzaldo A, Zompetti C, Vich JM. 1991. Dimethyl sulfoxide inhibits human immunodeficiency virus production in vitro. Intervirology 32:59–64.

Viza D, Aranda-Anzaldo A, Ablashi D, Kramarsky B. 1992. HHV-6 inhibition by two polar compounds. Antiviral Res 18:27–38.

Wykes SM, Krawetz SA. 2003. The structural organization of sperm chromatin. J Biol Chem 278:29471–29477.

Wykes SM, Nelson JE, Visscher DW, Djakiew D, Krawetz SA. 1995. Coordinate expression of the PRM1, PRM2, and TNP2 multigene locus in human testis. DNA Cell Biol 14:155–161.